



Splitting probabilities and mean first-passage times across multiple thresholds of jump-and-drift transition paths

Giulio Calvani ¹ and Paolo Perona ^{1,2}

¹Platform of Hydraulic Constructions (PL-LCH), IIC, School of Architecture, Civil and Environmental Engineering, EPFL, Lausanne 1015, Switzerland

²School of Engineering, Institute for Infrastructure and Environment, University of Edinburgh, Edinburgh EH9 3FG, United Kingdom



(Received 9 December 2022; revised 7 June 2023; accepted 11 September 2023; published 3 October 2023)

We apply stochastic-trajectory analysis to derive exact expressions for the mean first-passage times of jump-and-drift transition paths across two or more consecutive thresholds. We perform the analysis of the crossing statistics in terms of dimensionless quantities and show that, for particles starting between two thresholds, such statistics are directly related to the probability of not crossing one threshold and to the splitting probability of crossing the second one. We additionally derive a relationship for the mean first-passage time of the transition paths crossing two consecutive thresholds for particles starting outside them. The results are relevant to several physical and engineering applications including the case of flow discharge in fluvial environments, which is shown.

DOI: [10.1103/PhysRevE.108.044105](https://doi.org/10.1103/PhysRevE.108.044105)

I. INTRODUCTION

Several works in the literature have focused on the crossing statistics of stochastic processes subject to different noise sources ([1–3]). Among the crossing statistics, the Mean First Passage Time (henceforth referred to as MFPT) is the average time the process takes to reach a lower, X_1 , or an upper, X_2 , threshold for the first time when starting from a certain state, x_0 . The MFPT is of interest for many applications, ranging from biology [4] and economics [5] to physics [6] and chemistry [7]. Many authors derived exact expressions for the MFPT of different stochastic processes [8,9]. Among them, Laio *et al.* [10] investigated the MFPT of jump processes with negative drift across one threshold.

In nature, several processes show the presence of two (or even more) different boundaries. Specifically, these are processes for which the inferior threshold may be critical for triggering other types of dynamics [10,11]. For example, air temperature and day length (photoperiod) govern the relative time for flowering [12], vegetation budbreak [13], and algal blooming [14]. Another example is represented by the bedload and suspended transport of sediment in water courses (and therefore the morphological reworking due to erosion or deposition), which initiates only when the average bed shear stress, and therefore the discharge (i.e., the Shields stress [15]), is above (or below) a critical value.

The higher threshold may have either a physical meaning for biological (e.g., plant stress) and chemical (e.g., protein accumulation) processes or a statistical meaning (e.g., moving

boundary for Peak Over Threshold analysis [11]). Therefore, it is of interest to know the MFPT of only those trajectories that consecutively cross the lower, X_1 , (upper, X_2) threshold and the upper (lower) one, when the starting point of the transition path is below (above) the lower (upper) threshold, that is, $x_0 < X_1$ or $x_0 > X_2$, respectively (Fig. 1). To our knowledge, the continuous crossing of two or even more thresholds has been seldom investigated, with particular focus on the transition paths of rare events between metastable states in chemistry and physics, only [16,17]. When the presence of two thresholds is accounted for and the initial state, x_1 , lies between the two thresholds (i.e., $X_1 \leq x_1 \leq X_2$), the concept of crossing only one threshold is known in the literature as *splitting* or *hitting probability* [3]. Recently, the splitting probability has been investigated by involving pseudo-Green functions in diffusive processes [18] and by considering the asymptotic regime in symmetric jump processes [19,20] in the particular case of $X_1 = 0$.

In this work, we study the splitting probability and the MFPT across two thresholds of processes driven by white shot noise and deterministic drift, in consideration of their popular use as a proxy model of several physical, environmental, and socioeconomic processes [1–3,10,21–23]. First, we derive exact relationships for the splitting probability and the MFPT of trajectories starting from x_1 within the interval $[X_1, X_2]$. Then a global relationship for the consecutive crossing MFPT of two thresholds, henceforth named 2tMFPT, is formulated. As a result, we show that the quantity 2tMFPT is directly related to the crossing probability of the first threshold.

The paper is organized as follows. In Sec. II we describe the dynamics of the process by recalling previous findings and then introduce the dimensionless formulation, which will be used for further analysis and calculations. In Sec. III we derive the expressions for the splitting probability, in

Published by the American Physical Society under the terms of the [Creative Commons Attribution 4.0 International](https://creativecommons.org/licenses/by/4.0/) license. Further distribution of this work must maintain attribution to the author(s) and the published article's title, journal citation, and DOI.

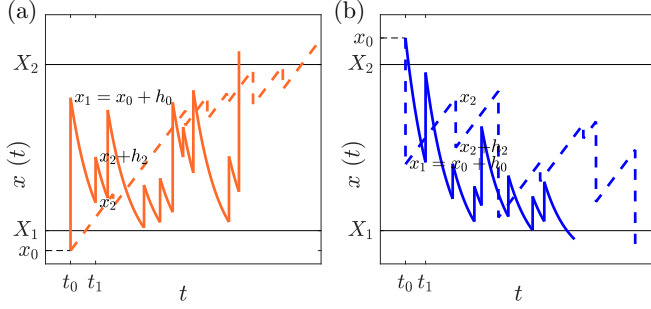


FIG. 1. Starting from x_0 , the process crosses the closer threshold either instantaneously with a jump or continuously during the first time interval, t_1 . Then it evolves in the interval $[X_1, X_2]$ starting from x_1 , ultimately crossing the other threshold. The continuous line refers to a process with negative drift and positive jumps. The dashed line shows a trajectory for a process with positive drift and negative jumps. Points x_1 , x_2 , and x_2+h_2 are highlighted for two trajectories, only. (a) Starting from $x_0 \leq X_1$, the trajectories cross the upper threshold, X_2 , without having crossed X_1 again. (b) Starting from $x_0 \geq X_2$, the trajectories crosses the lower threshold, X_1 , avoiding a second cross of the upper one, X_2 .

the case of constant and linear drift, and the comparison to numerical data from Monte Carlo simulations. The corresponding MFPT of crossing either one of the thresholds is formulated in Sec. IV, with a comparison to Monte Carlo simulations. The relationships for the 2tMFPT are proposed in Sec. IV, together with a practical application of the proposed framework for river flow analysis. Conclusions are drawn in Sec. V.

II. DYNAMICS OF THE SYSTEM

We consider processes whose dynamical evolution is governed by the following Langevin equation:

$$\frac{d x(t)}{d t} = f(x) + \zeta(t), \quad (1)$$

where $x = x(t) \geq 0$ is the state variable, t is time, $f(x)$ describes the deterministic drift, and $\zeta(t)$ is white shot noise, with exponentially distributed time intervals, τ_i , between jumps with mean $1/\lambda$ [i.e., $\psi_\tau(\tau_i) = \lambda e^{-\lambda\tau_i}$] and exponentially distributed jumps, h_i , with mean equal to $1/\gamma$ [i.e., $\psi_h(h_i) = |\gamma| e^{-\gamma h_i}$]. The absolute value in the jump height distribution, ψ_h , accounts for negative jumps in processes with positive drift [$f(x) \geq 0$]. Indeed, the analysis of threshold crossing in processes involving $f(x)\gamma \leq 0$ presents some drawbacks. In this case, the process admits an asymptotically stable point, x_s , in $x = 0$ ($x_s \rightarrow \infty$), according to the negative (positive) signs of γ and $f(x)$. Provided that the starting point is appropriately located [$x_0 \geq X_2$ or $x_0 \leq X_1$, for negative and positive $f(x)$, respectively], the 2tMFPT problem may still be solved. However, after the crossing of the closer threshold, the splitting probability of passing the uncrossed threshold simplifies to 1. As a matter of fact, in both cases, the problem reduces to finding the MFPT across the farthest threshold. In the opposite case, when the starting point lies on the same side of the asymptotically stable point with respect to the closer

threshold [$x_0 \leq X_2$ or $x_0 \geq X_1$, for negative and positive $f(x)$, respectively], the process is forced to move towards x_s , and may never cross either one of the thresholds. In this case, the 2tMFPT does not admit a solution.

For the process being considered, the probability density function of the starting point, $p(x_0)$, coincides with that of the unbounded process, which may be retrieved from the forward Chapman-Kolmogorov equation. This equation can be solved only in the case of negative drift [1,10,24], but this does not limit our analysis concerning the splitting probabilities and the mean first-passage time. In the following, the superscript \pm refers to the sign of the drift function. For $f(x) < 0$, a relationship for $p^-(x_0)$ reads

$$p^-(x_0) = -\frac{C}{f(x_0)} e^{-\gamma x_0 - \lambda \int_{x_0}^{\infty} \frac{du}{f(u)}}, \quad (2)$$

where C is a constant of integration which solves the condition $\int_0^\infty dx_0 p^-(x_0) = 1$ [1,10].

Let us now focus on the processes doing the first crossing via an instantaneous jump at $t = t_0$, that is, from x_0 to x_1 [see the continuous and dashed-dotted lines in Fig. 1(a) and Fig. 1(b), respectively]. For these trajectories, in the case of negative drift, the probability density function, $p_0^-(x_1)$, of the arrival points, x_1 , following a jump from the starting point, x_0 , can be simply obtained by considering that x_0 lies below the lower threshold, X_1 . The relationship may be straightforwardly derived via the integro-differential relationship

$$p_0^-(x_1) = -\frac{\partial}{\partial x_1} \int_0^{x_1} dx_0 p^-(x_0) |\gamma| e^{-\gamma(x_1-x_0)}. \quad (3)$$

Now we may proceed to consider the exit problem from the interval $[X_1 - X_2]$, when starting from x_1 . In this regard, we first need to derive a relationship for the splitting probability of only those trajectories that cross one boundary without touching the second one. For the splitting probability, we use the notation $\pi_k^\pm(t, x_1)$, which defines the probability, up to the time t , that the trajectories starting from x_1 exited from the threshold X_k without having passed the other threshold. In our notation, either sign of the superscript \pm refers to the sign of the drift of the $f(x_1)$ function.

According to the notation of Fig. 1, the statistical-trajectory analysis allows us to write the recursive equation relating the splitting probability, $\pi_k^\pm(t, x_1)$, of crossing the threshold X_k starting from x_1 , to the splitting probability, $\pi_k^\pm(t, x_2 + h_2)$, of crossing the same threshold starting from $x_2 + h_2$ (Fig. 1). In the Appendixes, we show that $\hat{\pi}_k^\pm(s, x_1)$, that is, the Laplace transform of $\pi_k^\pm(t, x_1)$, obeys the differential equation

$$\frac{\partial^2 \hat{\pi}_k^\pm(s, x_1)}{\partial x_1^2} + \left(\frac{f'(x_1) - \lambda - s}{f(x_1)} - \gamma \right) \frac{\partial \hat{\pi}_k^\pm(s, x_1)}{\partial x_1} + \frac{s\gamma}{f(x_1)} \hat{\pi}_k^\pm(s, x_1) = 0 \quad (4)$$

with $f'(x_1) = df(x_1)/dx_1$ and boundary conditions depending on the type of process (positive or negative drift) and on the threshold of interest:

$$\hat{\pi}_k^\pm(s, x_1) \Big|_{x_1=\begin{cases} X_2 \\ X_1 \end{cases}} = \delta[x_1 - X_k], \quad (5)$$

$$\left. \frac{\partial \hat{\pi}_k^\pm(s, x_1)}{\partial x_1} \right|_{x_1=\{X_1, X_2\}} = \frac{\lambda + s}{f(x_1)} \hat{\pi}_k^\pm(s, x_1) \Big|_{x_1=\{X_1, X_2\}} - \delta[x_1 - X_k] \frac{\lambda}{f(x_1)} \Big|_{x_1=\{X_1, X_2\}}, \quad (6)$$

where $\delta[\cdot]$ is the Kronecker's delta function, being equal to 1 when the argument in brackets is null, and zero otherwise. The coordinate of the boundary condition follows the \pm sign of the drift function. From $\hat{\pi}_1^\pm(s, x_1)$ and $\hat{\pi}_2^\pm(s, x_1)$, an expression for the Laplace-transform survivor function $\hat{\mathcal{F}}^\pm(s, x_1)$ by definition reads [1,25]

$$\hat{\mathcal{F}}^\pm(s, x_1) = 1 - \hat{\pi}_1^\pm(s, x_1) - \hat{\pi}_2^\pm(s, x_1). \quad (7)$$

The survivor function, $\mathcal{F}^\pm(t, x_1)$, and its Laplace transform, $\hat{\mathcal{F}}^\pm(s, x_1)$, represent the probability that the process has not crossed either threshold up to time t , or before the complex frequency s , respectively. An important novelty of this work is that we are interested in the survivor function of only those trajectories that have not crossed the threshold k . For these transition paths, we found that one can write the survivor function, $\hat{\mathcal{F}}_k^\pm(s, x_1)$, as

$$\hat{\mathcal{F}}_k^\pm(s, x_1) = 1 - \frac{\hat{\pi}_k^\pm(s, x_1)}{\hat{\pi}_k^\pm(s, x_1)|_{s=0}}, \quad (8)$$

where the denominator $\hat{\pi}_k^\pm(s, x_1)|_{s=0}$ allows for the fraction on the right-hand side to be equal to 1 when $s \rightarrow 0$ [3]. Equation (8) implies that the survived trajectories either still lie in the interval (X_1, X_2) or have already crossed the other threshold. The quantity $\hat{\pi}_k^\pm(0, x_1)$ may be simply obtained by substituting $s = 0$ in Eq. (4), thus yielding the differential equation:

$$\frac{d^2 \hat{\pi}_k^\pm(0, x_1)}{dx_1^2} + \left(\frac{f'(x_1) - \lambda}{f(x_1)} - \gamma \right) \frac{d\hat{\pi}_k^\pm(0, x_1)}{dx_1} = 0 \quad (9)$$

with boundary conditions from Eqs. (5) and (6) evaluated in $s = 0$.

From the survivor function, $\hat{\mathcal{F}}_k^\pm(s, x_1)$, the MFPT, $T_k^\pm(x_1)$, can be obtained as [8,25]

$$T_k^\pm(x_1) = \left. \frac{\partial \hat{\mathcal{F}}_k^\pm(s, x_1)}{\partial s} \right|_{s=0} = \frac{-1}{\hat{\pi}_k^\pm(0, x_1)} \left. \frac{\partial \hat{\pi}_k^\pm(s, x_1)}{\partial s} \right|_{s=0}. \quad (10)$$

By combining Eqs. (4) and (10) one arrives at the ordinary differential equation for $T_k^\pm(x_1)$, which reads

$$\begin{aligned} \frac{d^2 T_k^\pm(x_1)}{dx_1^2} + \left(\frac{f'(x_1) - \lambda}{f(x_1)} - \gamma \right) \frac{dT_k^\pm(x_1)}{dx_1} \\ = \frac{\gamma}{f(x_1)} - \frac{1}{f(x_1) \hat{\pi}_k^\pm(0, x_1)} \frac{d\hat{\pi}_k^\pm(0, x_1)}{dx_1}. \end{aligned} \quad (11)$$

A short digression is in order here. Eq. (11) is essentially similar to those derived by Masoliver [Ref. [8], Eq. (A4)] and Laio *et al.* [Ref. [10], Eq. (12)], except for the term which explicitly accounts for the splitting probability. In both

their approaches, the splitting probability may be considered constant and equal to 1, such that its derivative is null and the last term on the right-hand side of Eq. (11) canceled out. Specifically, Masoliver [8] did not distinguish between the exit from above X_2 or below X_1 , whereas Laio *et al.* [10] accounted for the presence of one threshold at a time and the crossing trajectories could wander freely before reaching it. Equation (11) requires two boundary conditions which may be calculated from Eqs. (5) and (6) by following the same procedure as above [Eq. (10)]. The obtained expressions for the boundary conditions read

$$\begin{aligned} T_k^\pm(x_1) \Big|_{x_1=\{X_1, X_2\}} &= 0, \\ \frac{dT_k^\pm(x_1)}{dx_1} \Big|_{x_1=\{X_1, X_2\}} &= \frac{\lambda T_k^\pm(x_1) - 1}{f(x_1)} \Big|_{x_1=\{X_1, X_2\}}. \end{aligned} \quad (12)$$

In the case of monomial forms of the drift function [i.e., $f(x) = \pm\beta x^a$, with $a \geq 0$], the problem may be approached in a dimensionless way by noticing that the quantity $|\gamma|^{a-1} \beta^{-1}$ represents a characteristic timescale of the process. Accordingly, we can write $\tilde{T}_k^\pm(z_1) = \beta |\gamma|^{1-a} T_k^\pm(z_1)$, with dimensionless variable $z = |\gamma|x$, and introduce the dimensionless thresholds $Z_k = |\gamma|X_k$, the Laplace frequency $\tilde{s} = |\gamma|^{a-1} \beta^{-1} s$, and the parameter $\alpha = \lambda |\gamma|^{a-1} \beta^{-1}$.

III. SPLITTING PROBABILITY

The solution of Eq. (9) is straightforward and reads

$$\hat{\pi}_k^\pm(0, x_1) = C_{\pi_{k1}}^\pm + C_{\pi_{k2}}^\pm \int_{x_1}^{X_1} dx \frac{1}{f(x)} e^{\gamma x + \lambda \int_{x_1}^x \frac{du}{f(u)}}. \quad (14)$$

The solution in Eq. (14), as well as that of Eq. (4), depends on the shape of the drift function $f(x)$. It is remarkable to note that, in the case the drift is represented by an even function, it is possible to write the solutions in a more compact way, by taking advantage of the substitution $x \rightarrow -x$ in Eq. (1). In the following, we focus on the cases of constant [$f(x) = \pm\beta$] and linear [$f(x) = \pm\beta x$] drift functions [10,24], by considering the dimensionless quantities previously defined.

In the case of constant drift, Eq. (4) reduces to a damped-vibration-like differential equation, and its solution reads

$$\hat{\pi}_k^\pm(\tilde{s}, z_1) = e^{\pm \frac{\tilde{s}}{2}(\alpha + \tilde{s} - 1)} \left(C_{\pi_{k1}}^\pm(\tilde{s}) e^{\frac{\tilde{s}}{2} \Delta} + C_{\pi_{k2}}^\pm(\tilde{s}) e^{-\frac{\tilde{s}}{2} \Delta} \right) \quad (15)$$

with $\Delta = \sqrt{(\alpha + \tilde{s} - 1)^2 + 4\tilde{s}}$. In $\tilde{s} = 0$, Δ reduces to $\alpha - 1$, and the solution simplifies to

$$\hat{\pi}_k^\pm(0, z_1) = C_{\pi_{k2}}^\pm(0) + C_{\pi_{k1}}^\pm(0) e^{\pm(\alpha-1)z_1}, \quad (16)$$

where the integration constants depend on the thresholds and have to be chosen according to the sign of the drift function.

In the case of linear drift, Eq. (4) reduces to a degenerate hypergeometric equation, whose solution may be written as

$$\begin{aligned} \hat{\pi}_k^\pm(\tilde{s}, z_1) = C_{\pi_{k1}}^\pm(\tilde{s}) {}_1F_1[\mp\tilde{s}; 1 \mp \alpha \mp \tilde{s}; \mp z_1] \\ + C_{\pi_{k2}}^\pm(\tilde{s}) (\mp z_1)^{\pm(\alpha+\tilde{s})} {}_1F_1[\pm\alpha; 1 \pm \alpha \pm \tilde{s}; \mp z_1], \end{aligned} \quad (17)$$

where ${}_1F_1[\cdot; \cdot; \cdot]$ represents the Kummer's confluent hypergeometric function [26]. In $\tilde{s} = 0$, the relationship

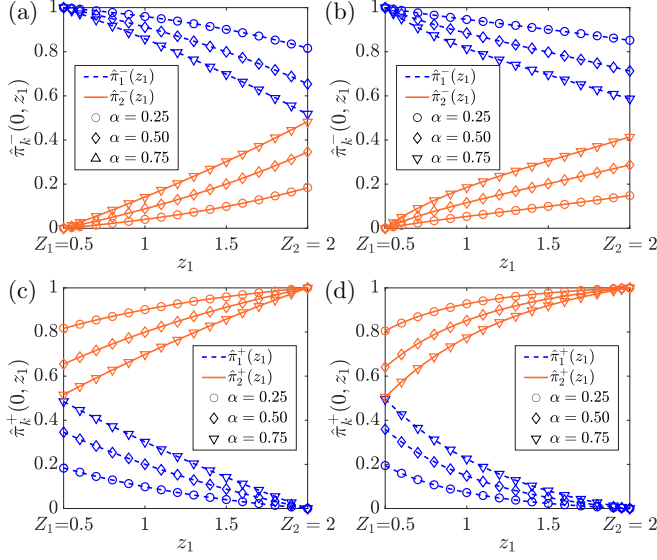


FIG. 2. Splitting probabilities, $\hat{\pi}_k^\pm(0, z_1)$, in processes with different sign and form (constant or linear) of the drift function, at varying the starting point z_1 , given $Z_1 \leq z_1 \leq Z_2$, for some values of the parameter α . Dashed blue (dark gray) and continuous orange (light gray) lines refer to the crossing of the lower and the upper thresholds, respectively. Points are data from Monte Carlo simulations. (a) Negative constant drift; (b) negative linear drift; (c) positive constant drift; (d) positive linear drift.

reduces to

$$\hat{\pi}_k^\pm(0, z_1) = C_{\pi_{k1}}^\pm(0) + C_{\pi_{k2}}^\pm(0) (-1)^\alpha \times (\Gamma[1 \pm \alpha] \mp \alpha \Gamma[\pm \alpha; \pm z_1]), \quad (18)$$

where $\Gamma[\cdot]$ and $\Gamma[\cdot; \cdot]$ are the gamma and the incomplete gamma functions, respectively [26]. In Eqs. (15)–(18) the integration constants $C_{\pi_{ki}}(\bar{s})$ may be determined based on the boundary conditions given in Eqs. (5) and (6), evaluated in $\bar{s} = 0$ when necessary. Figure 2 shows the comparison of the derived formulations [Eqs. (16) and (18)] to data from Monte Carlo simulations for different values of the parameters α and given values of the thresholds Z_k . Both the cases of positive and negative drift are shown as well.

The difference between constant and linear drift is highlighted in Fig. 3, which shows the shape of the splitting probability $\hat{\pi}_1^-(0, z_1)$ when varying the starting point, z_1 , and the upper threshold, Z_2 , for a fixed value of the lower threshold, $Z_1 = 0.5$, and two values of α .

IV. MEAN FIRST-PASSAGE TIME

The solution of Eq. (11) reads

$$T_k^\pm(x_1) = C_{T_{k1}}^\pm + \int^{x_1} dx \frac{1}{f(x)} e^{\gamma x + \lambda \int^x \frac{du}{f(u)}} \times \left[C_{T_{k2}}^\pm + \int^x dy f(y) e^{-\gamma y - \lambda \int^y \frac{du}{f(u)}} \times \left(\frac{\gamma}{f(y)} - \frac{1}{f(y) \hat{\pi}_k^\pm(0, y)} \frac{d\hat{\pi}_k^\pm(0, y)}{dy} \right) \right], \quad (19)$$

whose closed-form expression depends on the forms of the splitting probability and its derivative with respect to x_1 ,

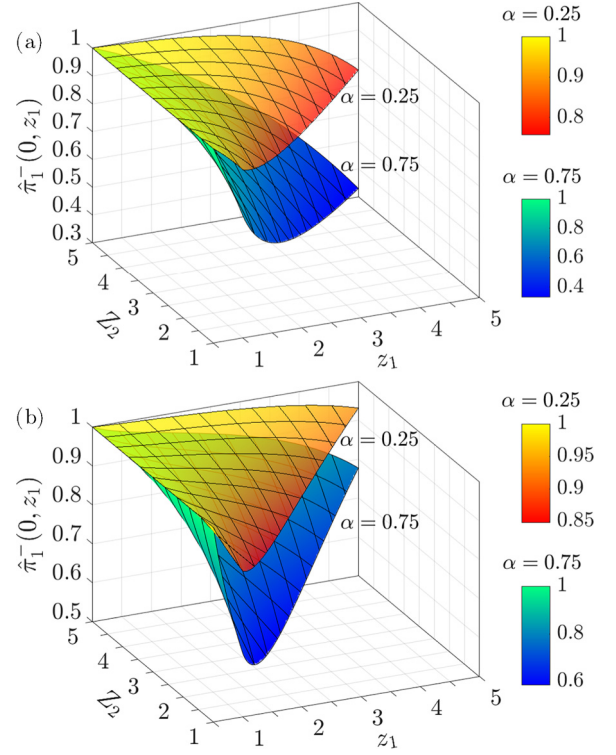


FIG. 3. Splitting probabilities $\hat{\pi}_1^-(0, z_1)$ for $Z_1 = 0.5$ at varying the starting point, z_0 , and the upper threshold, Z_2 , for $\alpha = 0.25$ (red-yellow shade) and $\alpha = 0.75$ (blue-green shade) in two processes with negative constant [$f(x) = -\beta$, panel a] and linear [$f(x) = -\beta x$, panel b] drift.

which are basically related to the drift function $f(x_1)$. Despite being elegant, Eq. (19) requires that a double integral is solved, which may not be a practicable solution in many instances. In this case, it is easier to obtain the solution via Eq. (10). For the particular cases of constant and linear drifts presented in this work, the closed-form expression in terms of dimensionless quantities may be retrieved from the corresponding relationships for the splitting probability, by considering Eq. (10). In the case of constant drift, from Eqs. (15) and (16) one may find

$$\begin{aligned} \tilde{T}_k^\pm(z_1) &= -\frac{1 + \alpha z_1}{1 - \alpha z_1} \\ &\mp \frac{\frac{z_1}{2} C_{\pi_{k1}}^\pm(0) \pm C_{\pi_{k1}}^{\pm'}(0)}{C_{\pi_{k1}}^\pm(0) + C_{\pi_{k2}}^\pm(0) e^{(1-\alpha)z_1}} \\ &\mp \frac{\frac{z_1}{2} C_{\pi_{k2}}^\pm(0) \pm C_{\pi_{k2}}^{\pm'}(0)}{C_{\pi_{k1}}^\pm(0) e^{(\alpha-1)z_1} + C_{\pi_{k2}}^\pm(0)}, \end{aligned} \quad (20)$$

where $C_{\pi_{ki}}^{\pm'}(0) = \frac{\partial C_{\pi_{ki}}^\pm(\bar{s})}{\partial \bar{s}} \Big|_{\bar{s}=0}$.

In the case of linear drift, from Eqs. (17) and (18) we derive

$$\begin{aligned} \tilde{T}_k^\pm(z_1) &= -\frac{1}{\hat{\pi}_k^\pm(0, z_1)} \left(C_{\pi_1}^{\pm'}(0) + (\mp z_1)^{\pm \alpha} \right. \\ &\times {}_1F_1[\pm \alpha; 1 \pm \alpha; \mp z_1] (C_{\pi_2}^{\pm'}(0) \pm C_{\pi_2}^\pm(0) \log[\mp z_1]) \\ &\left. + C_{\pi_2}^\pm(0) (\mp z_1)^{\pm \alpha} \frac{\alpha z_1}{(1 \pm \alpha)^2} \right) \end{aligned}$$

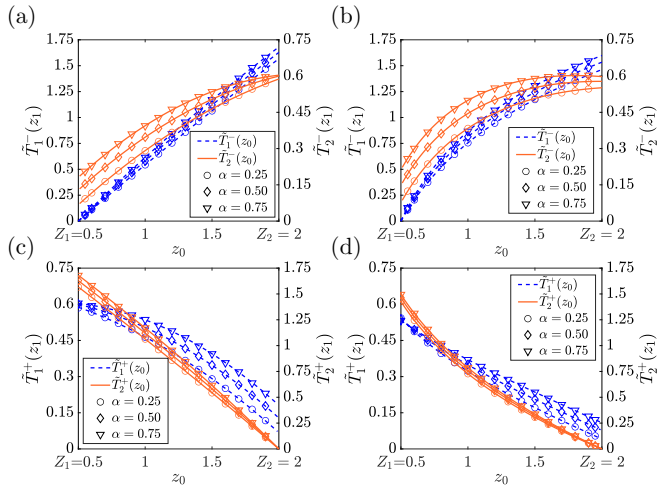


FIG. 4. Dimensionless MFPTs, $\tilde{T}_k^\pm(z_1)$, in processes with different sign and form (constant or linear) of the drift function, for varying starting point z_1 , given $Z_1 \leq z_1 \leq Z_2$, for some values of the parameter α . Dashed blue (dark gray) and continuous orange (light gray) lines refer to the crossing of the lower and the upper thresholds, respectively. Points are data from Monte Carlo simulations. (a) Negative constant drift; (b) negative linear drift; (c) positive constant drift; (d) positive linear drift.

$$\begin{aligned} & \times \Theta \left[\begin{array}{c|c} 1; 1 & 1 \pm \alpha; 1 \pm \alpha \\ \hline 2 \pm \alpha & 2; 2 \pm \alpha \end{array} \middle| \mp z_1; \mp z_1 \right] \\ & \mp C_{\pi 1}(0) \frac{z_1}{1 \mp \alpha} \\ & \times \Theta \left[\begin{array}{c|c} 1; 1 & 0; 1 \\ \hline 1 & 2; 2 \pm \alpha \end{array} \middle| \mp z_1; \mp z_1 \right], \quad (21) \end{aligned}$$

where $\Theta \left[\begin{array}{c|c} \cdot & \cdot \\ \hline \cdot & \cdot \end{array} \middle| \cdot; \cdot \right]$ is a Kampé de Fériet-like function [27,28].

The comparison of the derived formulations [Eqs. (20) and (21)] to data from Monte Carlo simulations is shown in Fig. 4, according to different values of the parameter α and given values of the thresholds Z_k , for both cases of positive and negative drifts. Figure 5 shows the shape of $\tilde{T}_2^\pm(z_1)$ for two processes with constant and linear negative drift, at varying the starting point, z_1 , and the upper threshold, Z_2 , for a fixed value of the lower threshold, $Z_1 = 0.5$, and two values of α . As a result, the function $\tilde{T}_2^\pm(z_1)$ shows the presence of a local maximum by varying the initial state z_1 . Interestingly, the occurrence of the maximum is independent of the upper threshold Z_2 but depends on the dimensionless parameter α and the form of the drift function (e.g., constant or linear in panels a and b of Fig. 5, respectively).

Finally, a relationship for the 2tMFPT, ${}_2\tilde{T}_k^\pm(z_0)$, must be considered on a case-by-case basis. For processes with negative drift, a relationship for the ${}_2\tilde{T}_2^-(z_0)$, that is the MFPT of the transition path from below Z_1 to above Z_2 , may be calculated by considering the probability distribution function given in Eq. (3). In this case, we may write

$${}_2\tilde{T}_2^-(z_0) = \int_{Z_1}^{Z_2} dz_1 p_0^-(z_1) \tilde{T}_2^-(z_1). \quad (22)$$

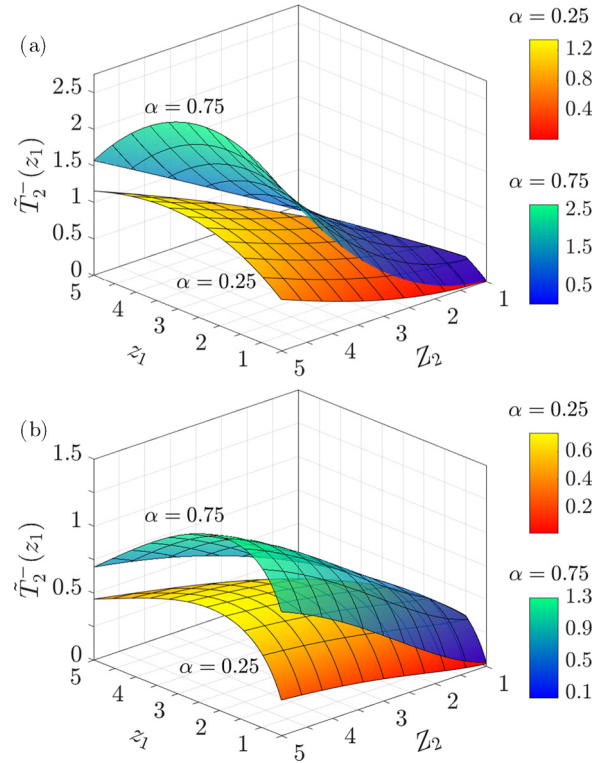


FIG. 5. Dimensionless MFPT $\tilde{T}_2^\pm(z_1)$ for $Z_1 = 0.5$ by varying the starting point, z_1 , and the upper threshold, Z_2 , for $\alpha = 0.25$ (red-yellow shade) and $\alpha = 0.75$ (blue-green shade). Results are shown for two processes with negative constant [$f(x) = -\beta$, panel a] and linear [$f(x) = -\beta x$, panel b] drift.

Such a relationship may not be written for processes with positive drift and crossing both the thresholds from above Z_2 , as a solution for $p_0^+(z_1)$ is missing [1,10,24]. However, when the first crossing occurs through a continuous path [see the dashed orange (light gray) line in Fig. 1(a) for positive drift, and the continuous blue (dark gray) line in Fig. 1(b) for negative drift], we may consider the first-crossed threshold as the starting point of the transition path, that is ${}_2\tilde{T}_1^+(Z_2) = \tilde{T}_1^+(Z_2)$ and ${}_2\tilde{T}_2^-(Z_1) = \tilde{T}_2^-(Z_1)$.

We tested Eq. (22) against flow data of the Thur River measured at the Adelfingen gauge station in Switzerland [top, Fig. 6(a)]. The corresponding stochastic process has an average jump height $\gamma^* = 153 \text{ m}^3\text{s}^{-1}$, linear decay coefficient $\beta^* = 0.0115 \text{ h}^{-1}$ and dimensionless parameter $\alpha = 0.318$. A sample of the modeled discharge process is shown in the bottom panel of Fig. 6(a). Figure 6(b) shows the comparison between measured and calculated durations for several combinations of the lower ($Z_1 = [0.5, 1, 2, 3]$) and upper ($Z_2 = [3, 4, 5, 6]$) dimensionless thresholds according to different trajectories. For the sake of comparison, the predicted ${}_2\tilde{T}_2^-(z_0)$ must account for the time interval in the data acquisition ($\Delta t = 1$ hour). In fact, every jump in the measured data occurs with a delay Δt with respect to the modeled process. As a result, the ${}_2\tilde{T}_2^-(z_0)$ must be increased by a quantity that accounts for the average number of jumps, that is, $\beta (Z_2 - Z_1 + 1) \Delta t$. The comparison shows good agreement for the predicted values of ${}_2\tilde{T}_2^-(z_0)$ ($R^2 = 0.806$).

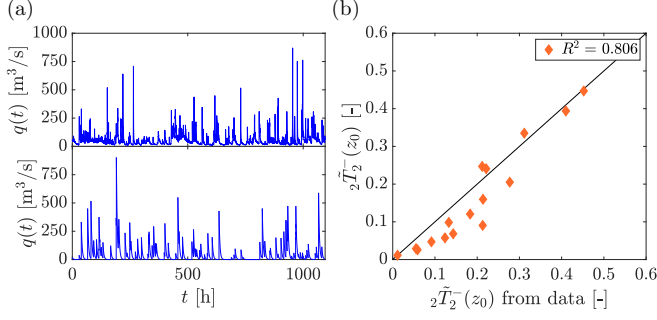


FIG. 6. Application of Eq. (22) to a two-month signal of measured flow discharge for the Thur River in Switzerland. (a) Flow measurements (upper panel) at the Andelfingen gauge station (CH) and one realization of the statistically equivalent compound Poisson process with linear drift (lower panel); (b) Comparison between predicted and measured dimensionless $2\bar{T}_2^-(z_0)$ based on different Z_1, Z_2 combinations.

V. CONCLUSIONS

The MFPT of the transition paths in jump processes with drift across two consecutive thresholds was studied, both in the cases of positive and negative drifts. We showed that the continuous crossing depends on the splitting probability, for which we derived a differential equation and solved it for the cases of constant and linear drifts. Based on the relationships for the splitting probability, we obtained closed-form expressions for the MFPT across one threshold and found integral relationships for the continuous cross of two consecutive thresholds. The relationships were tested against data from Monte Carlo simulations and real measurements of geophysical flows such as the river discharge.

ACKNOWLEDGMENTS

This research is carried out in the frame of the ‘‘UrbanTwin: An urban digital twin for climate action’’ project with the financial support of the ETH-Domain Joint Initiative program. The authors wish to thank Amilcare Porporato for fruitful discussions on the topic.

APPENDIX A: DIFFERENTIAL EQUATIONS FOR THE SPLITTING PROBABILITY

According to the notation of Fig. 1, we follow the procedure of Masoliver [Ref. [8], Eqs. (3.13)–(3.19)], by accounting for exponentially distributed intervals between jumps and jump heights, with ψ_t and ψ_h their probability distribution functions, respectively.

For the drift-driven crossing, one may write

$$\hat{\pi}_{\{1\}}^{\pm}(s, x_1) = e^{-s\bar{t}_1^{\pm}} \int_{\bar{t}_1^{\pm}}^{\infty} dt_1^* \psi_t(t_1^*) \mp \int_{x_1}^{X_2} dx_2 e^{-s\bar{t}_1^*} \frac{\psi_t(t_1^*)}{f(x_2)} \times \int_0^{\{X_1-x_2, X_2-x_2\}} dh_2 \psi_h(h_2) \hat{\pi}_{\{2\}}^{\pm}(s, x_2 + h_2), \quad (\text{A1})$$

where $t_1^* = t_1 - t_0$ and $\bar{t}_1^{\pm} = \int_{x_1}^{X_2} dx_2 \frac{1}{f(x_2)}$ represents the time at the drift-driven crossing, starting from x_1 .

Conversely, for the jump-driven crossing, one has

$$\hat{\pi}_{\{2\}}^{\pm}(s, x_1) = \mp \int_{x_1}^{\{X_2, X_1\}} dx_2 e^{-s\bar{t}_1^*} \frac{\psi_t(t_1^*)}{f(x_2)} \times \int_{\{X_1-x_2, X_2-x_2\}}^{\mp\infty} dh_2 \psi_h(h_2) \mp \int_{x_1}^{\{X_2, X_1\}} dx_2 e^{-s\bar{t}_1^*} \frac{\psi_t(t_1^*)}{f(x_2)} \times \int_0^{\{X_1-x_2, X_2-x_2\}} dh_2 \psi_h(h_2) \hat{\pi}_{\{1\}}^{\pm}(s, x_2 + h_2). \quad (\text{A2})$$

The partial derivative of (A1) and (A2) with respect to x_1 are

$$\frac{\partial \hat{\pi}_{\{1\}}^{\pm}(s, x_1)}{dx_1} = \frac{\lambda + s}{f(x_1)} \hat{\pi}_{\{2\}}^{\pm}(s, x_1) \mp \frac{-\lambda}{f(x_1)} \int_0^{\{X_1-x_1, X_2-x_1\}} dh_2 \psi_h(h_2) \hat{\pi}_{\{2\}}^{\pm}(s, x_1 + h_2) \quad (\text{A3})$$

and

$$\frac{\partial \hat{\pi}_{\{2\}}^{\pm}(s, x_1)}{dx_1} = \frac{\lambda + s}{f(x_1)} \hat{\pi}_{\{1\}}^{\pm}(s, x_1) \mp \frac{-\lambda}{f(x_1)} \left(\int_{\{X_1-x_1, X_2-x_1\}}^{\mp\infty} dh_2 \psi_h(h_2) + \int_0^{\{X_1-x_1, X_2-x_1\}} dh_2 \psi_h(h_2) \hat{\pi}_{\{1\}}^{\pm}(s, x_2 + h_2) \right). \quad (\text{A4})$$

Another partial derivation with respect to x_1 , integration by parts and reorganizations of terms by considering $|\gamma| = \mp\gamma$ for positive and negative drift, respectively, yield the same second-order differential equation [Eq. (4)]:

$$\frac{\partial^2 \hat{\pi}_k^{\pm}(s, x_1)}{\partial x_1^2} + \left(\frac{f'(x_1) - \lambda - s}{f(x_1)} - \gamma \right) \frac{\partial \hat{\pi}_k^{\pm}(s, x_1)}{\partial x_1} + \frac{s\gamma}{f(x_1)} \hat{\pi}_k^{\pm}(s, x_1) = 0. \quad (\text{A5})$$

The first boundary condition is obtained from Eq. (A1) by setting $x_1 = X_{\{2\}}$ and from Eq. (A2) by setting $x_1 = X_{\{1\}}$. This leads to the boundary condition shown in Eq. (5), which basically states that in processes with positive (negative) drift, the splitting probability of crossing the upper (lower) threshold, starting from the upper (lower) threshold itself, is 1.

The second boundary condition is obtained from Eq. (A3) by setting $x_1 = X_{\{1\}}$ and from Eq. (A4) by setting $x_1 = X_{\{2\}}$. The

physical meaning of such a boundary condition is unknown [8,9].

APPENDIX B: DIFFERENTIAL EQUATIONS FOR THE MEAN FIRST-PASSAGE TIME

An equation for the the MFPT, $T_k^\pm(x_1)$, may be obtained by considering that

$$T_k^\pm(x_1) = -\frac{1}{\hat{\pi}_k^\pm(0, x_1)} \left. \frac{\partial \hat{\pi}_k^\pm(s, x_1)}{\partial s} \right|_{s=0}. \tag{B1}$$

As a consequence, Eq. (A5), together with its boundary conditions [Eqs. (5) and (6)], can be divided by $\hat{\pi}_k^\pm(0, x_1)$ and changed of sign. Taking a partial derivative with respect to s , evaluating the obtained equation in $s = 0$, and considering Eq. (B1) lead to

$$\begin{aligned} \frac{d^2 T_k^\pm(x_1)}{dx_1^2} + \left(\frac{f'(x_1) - \lambda}{f(x_1)} - \gamma \right) \frac{dT_k^\pm(x_1)}{dx_1} \\ = \frac{\gamma}{f(x_1)} - \frac{1}{f(x_1)} \frac{d\hat{\pi}_k^\pm(0, x_1)}{\hat{\pi}_k^\pm(0, x_1) dx_1} \end{aligned} \tag{B2}$$

and the boundary conditions given in Eqs. (12) and (13).

APPENDIX C: INTEGRATION CONSTANTS

The relationships for the integration constants are given in the following sections according to the type of drift. For the sake of clarity, we here recall some notations: $\Gamma[\cdot]$ is the gamma function, ${}_1F_1[\cdot; \cdot; \cdot]$ is the Kummer’s confluent hypergeometric function and ${}_1\tilde{F}_1[\cdot; b; \cdot] = \Gamma[b] {}_1F_1[\cdot; b; \cdot]$ is the regularized confluent hypergeometric function. Additionally, for the cases of constant drift [i.e., $f(x) = \pm\beta$], we define the quantity $\Delta = \sqrt{(\alpha + \tilde{s} - 1)^2 + 4\tilde{s}}$. When necessary, the relationships for the integration constants must be evaluated in $\tilde{s} = 0$.

1. Positive constant drift

In the case of positive constant drift [i.e., $f(x) = \beta$], the integration constants for Eq. (15) are

$$C_{\pi_{11}}^+(\tilde{s}) = \frac{2\alpha e^{-\frac{Z_1}{2}(\alpha+\tilde{s}-1-\Delta)}}{(\alpha + \tilde{s} + 1 - \Delta)e^{\Delta Z_1} - (\alpha + \tilde{s} + 1 + \Delta)e^{\Delta Z_2}}, \tag{C1}$$

$$C_{\pi_{12}}^+(\tilde{s}) = -\frac{2\alpha e^{\Delta Z_2 - \frac{Z_1}{2}(\alpha+\tilde{s}-1-\Delta)}}{(\alpha + \tilde{s} + 1 - \Delta)e^{\Delta Z_1} - (\alpha + \tilde{s} + 1 + \Delta)e^{\Delta Z_2}}, \tag{C2}$$

$$C_{\pi_{21}}^+(\tilde{s}) = -\frac{(\alpha + \tilde{s} + 1 + \Delta) e^{-\frac{Z_2}{2}(\alpha+\tilde{s}-1+\Delta)}}{(\alpha + \tilde{s} + 1 - \Delta)e^{\Delta Z_1} - (\alpha + \tilde{s} + 1 + \Delta)e^{\Delta Z_2}}, \tag{C3}$$

$$C_{\pi_{22}}^+(\tilde{s}) = \frac{(\alpha + \tilde{s} + 1 - \Delta)e^{\Delta Z_1 - \frac{Z_2}{2}(\alpha+\tilde{s}-1-\Delta)}}{(\alpha + \tilde{s} + 1 - \Delta)e^{\Delta Z_1} - (\alpha + \tilde{s} + 1 + \Delta)e^{\Delta Z_2}}. \tag{C4}$$

2. Negative constant drift

In the case of negative constant drift [i.e., $f(x) = -\beta$], the integration constants for Eq. (15) are

$$C_{\pi_{11}}^-(\tilde{s}) = \frac{(\alpha + \tilde{s} + 1 - \Delta) e^{\frac{Z_1}{2}(\alpha+\tilde{s}-1+\Delta)}}{(\alpha + \tilde{s} + 1 - \Delta)e^{\Delta Z_1} - (\alpha + \tilde{s} + 1 + \Delta)e^{\Delta Z_2}}, \tag{C5}$$

$$C_{\pi_{12}}^-(\tilde{s}) = \frac{(\alpha + \tilde{s} + 1 + \Delta)e^{\Delta Z_2 + \frac{Z_1}{2}(\alpha+\tilde{s}-1+\Delta)}}{(\alpha + \tilde{s} + 1 - \Delta)e^{\Delta Z_1} - (\alpha + \tilde{s} + 1 + \Delta)e^{\Delta Z_2}}, \tag{C6}$$

$$C_{\pi_{21}}^-(\tilde{s}) = -\frac{2\alpha e^{\frac{Z_2}{2}(\alpha+\tilde{s}-1+\Delta)}}{(\alpha + \tilde{s} + 1 - \Delta)e^{\Delta Z_1} - (\alpha + \tilde{s} + 1 + \Delta)e^{\Delta Z_2}}, \tag{C7}$$

$$C_{\pi_{22}}^-(\tilde{s}) = \frac{2\alpha e^{\Delta Z_1 + \frac{Z_2}{2}(\alpha+\tilde{s}-1+\Delta)}}{(\alpha + \tilde{s} + 1 - \Delta)e^{\Delta Z_1} - (\alpha + \tilde{s} + 1 + \Delta)e^{\Delta Z_2}}. \tag{C8}$$

3. Positive linear drift

In the case of positive linear drift [i.e., $f(x) = \beta x$], the integration constants for Eq. (17) are

$$\begin{aligned} C_{\pi_{11}}^+(\tilde{s}) = \frac{\alpha \sin[\pi(\alpha + \tilde{s})]}{\pi(\alpha + \tilde{s})Z_1} {}_1F_1[\alpha; \tilde{s} + \alpha + 1; -Z_2] \left((\alpha - 1) {}_1\tilde{F}_1[-\tilde{s}; -\tilde{s} - \alpha + 2; -Z_1] {}_1\tilde{F}_1 \right. \\ \times [\alpha; \tilde{s} + \alpha + 1; -Z_2] + \frac{\alpha + \tilde{s} + Z_1}{Z_1} {}_1\tilde{F}_1[-\tilde{s}; -\tilde{s} - \alpha + 1; -Z_1] {}_1\tilde{F}_1[\alpha; \tilde{s} + \alpha + 1; -Z_2] \\ \left. - \alpha \left(\frac{Z_1}{Z_2} \right)^{\alpha+\tilde{s}} {}_1\tilde{F}_1[-\tilde{s}; -\tilde{s} - \alpha + 1; -Z_2] {}_1\tilde{F}_1[\alpha + 1; \tilde{s} + \alpha + 2; -Z_1] \right)^{-1}, \end{aligned} \tag{C9}$$

$$\begin{aligned} C_{\pi_{12}}^+(\tilde{s}) = \frac{\alpha \sin[\pi(\alpha + \tilde{s})]}{\pi(\alpha + \tilde{s})} {}_1F_1[-\tilde{s}; -\tilde{s} - \alpha + 1; -Z_2] \left[(\alpha - 1) \left(\frac{Z_2}{Z_1} \right)^{\alpha+\tilde{s}} {}_1\tilde{F}_1[-\tilde{s}; -\tilde{s} - \alpha + 2; -Z_1] {}_1\tilde{F}_1[\alpha; \tilde{s} + \alpha + 1; -Z_2] \right. \\ \left. + \frac{\alpha + \tilde{s} + Z_1}{Z_1} \left(\frac{Z_2}{Z_1} \right)^{\alpha+\tilde{s}} {}_1\tilde{F}_1[-\tilde{s}; -\tilde{s} - \alpha + 1; -Z_1] {}_1\tilde{F}_1[\alpha; \tilde{s} + \alpha + 1; -Z_2] - \alpha {}_1\tilde{F}_1[-\tilde{s}; -\tilde{s} - \alpha + 1; -Z_2] {}_1\tilde{F}_1 \right. \\ \left. \times [\alpha + 1; \tilde{s} + \alpha + 2; -Z_1] \right]^{-1}, \end{aligned} \tag{C10}$$

$$C_{\pi_2 1}^+(\tilde{s}) = \alpha {}_1F_1[\alpha + 1; \tilde{s} + \alpha + 2; -Z_1] \left[(\alpha + \tilde{s} + 1) \left(\frac{Z_2}{Z_1} \right)^{\alpha + \tilde{s}} {}_1F_1[\alpha; \tilde{s} + \alpha + 1; -Z_2] \right. \\ \left. \times \left(\frac{(\alpha - 1) {}_1F_1[-\tilde{s}; -\tilde{s} - \alpha + 2; -Z_1]}{\alpha + \tilde{s} - 1} - \frac{\alpha + \tilde{s} + Z_1}{Z_1} {}_1F_1[-\tilde{s}; -\tilde{s} - \alpha + 1; -Z_1] \right) \right. \\ \left. + \alpha {}_1F_1[-\tilde{s}; -\tilde{s} - \alpha + 1; -Z_2] {}_1F_1[\alpha + 1; \tilde{s} + \alpha + 2; -Z_1] \right]^{-1}, \quad (C11)$$

$$C_{\pi_2 2}^+(\tilde{s}) = (\alpha + \tilde{s} + 1) \left(\frac{\alpha - 1}{\alpha + \tilde{s} - 1} {}_1F_1[-\tilde{s}; -\tilde{s} - \alpha + 2; -Z_1] - \frac{\alpha + \tilde{s} + Z_1}{Z_1} {}_1F_1[-\tilde{s}; -\tilde{s} - \alpha + 1; -Z_1] \right) \\ \times \left[\alpha (-Z_1)^{\alpha + \tilde{s}} {}_1F_1[-\tilde{s}; -\tilde{s} - \alpha + 1; -Z_2] {}_1F_1[\alpha + 1; \tilde{s} + \alpha + 2; -Z_1] \right. \\ \left. + (-Z_2)^{\alpha + \tilde{s}} {}_1F_1[\alpha; \tilde{s} + \alpha + 1; -Z_2] \left(\frac{\alpha + \tilde{s} + Z_1}{Z_1} {}_1F_1[-\tilde{s}; -\tilde{s} - \alpha + 1; -Z_1] \right. \right. \\ \left. \left. - \frac{\alpha - 1}{\alpha + \tilde{s} - 1} {}_1F_1[-\tilde{s}; -\tilde{s} - \alpha + 2; -Z_1] \right) \right]^{-1}. \quad (C12)$$

4. Negative linear drift

In the case of negative linear drift [i.e., $f(x) = -\beta x$], the integration constants for Eq. (17) are

$$C_{\pi_1 1}^-(\tilde{s}) = \alpha \frac{{}_1\tilde{F}_1[1 - \alpha; -\tilde{s} - \alpha + 2; Z_2]}{\Gamma[\tilde{s} + \alpha + 1]} \left[\left(\frac{Z_2}{Z_1} \right)^{\alpha + \tilde{s}} {}_1\tilde{F}_1[-\alpha; -\tilde{s} - \alpha + 1; Z_1] \right. \\ \left. \times \left(\frac{\alpha + \tilde{s} + Z_2}{Z_2} {}_1\tilde{F}_1[\tilde{s}; \tilde{s} + \alpha + 1; Z_2] - (\alpha + 1) {}_1\tilde{F}_1[\tilde{s}; \tilde{s} + \alpha + 2; Z_2] \right) \right. \\ \left. + \alpha {}_1\tilde{F}_1[\tilde{s}; \tilde{s} + \alpha + 1; Z_1] {}_1\tilde{F}_1[1 - \alpha; -\tilde{s} - \alpha + 2; Z_2] \right]^{-1}, \quad (C13)$$

$$C_{\pi_1 2}^-(\tilde{s}) = \frac{1}{\Gamma[-\tilde{s} - \alpha + 1]} ((\alpha + 1) Z_2 {}_1\tilde{F}_1[\tilde{s}; \tilde{s} + \alpha + 2; Z_2] - (\alpha + \tilde{s} + Z_2) {}_1\tilde{F}_1[\tilde{s}; \tilde{s} + \alpha + 1; Z_2]) \\ \times \left[Z_1^{-\alpha - \tilde{s}} {}_1\tilde{F}_1[-\alpha; -\tilde{s} - \alpha + 1; Z_1] \left((\alpha + 1) {}_1\tilde{F}_1[\tilde{s}; \tilde{s} + \alpha + 2; Z_2] - \frac{\alpha + \tilde{s} + Z_2}{Z_2} {}_1\tilde{F}_1[\tilde{s}; \tilde{s} + \alpha + 1; Z_2] \right) \right. \\ \left. - \alpha Z_2^{-\alpha - \tilde{s}} {}_1\tilde{F}_1[\tilde{s}; \tilde{s} + \alpha + 1; Z_1] {}_1\tilde{F}_1[1 - \alpha; -\tilde{s} - \alpha + 2; Z_2] \right]^{-1}, \quad (C14)$$

$$C_{\pi_2 1}^-(\tilde{s}) = \frac{1}{\alpha Z_2 \Gamma[\tilde{s} + \alpha + 1]} \left[\alpha \left(\frac{Z_1}{Z_2} \right)^{\alpha + \tilde{s}} \frac{{}_1\tilde{F}_1[\tilde{s}; \tilde{s} + \alpha + 1; Z_1] {}_1\tilde{F}_1[1 - \alpha; -\tilde{s} - \alpha + 2; Z_2]}{{}_1\tilde{F}_1[-\alpha; -\tilde{s} - \alpha + 1; Z_1]} + \frac{\alpha + \tilde{s} + Z_2}{Z_2} {}_1\tilde{F}_1[\tilde{s}; \tilde{s} + \alpha + 1; Z_2] \right. \\ \left. - (\alpha + 1) {}_1\tilde{F}_1[\tilde{s}; \tilde{s} + \alpha + 2; Z_2] \right]^{-1}. \quad (C15)$$

$$C_{\pi_2 2}^-(\tilde{s}) = -\alpha Z_2^{\alpha + \tilde{s}} \frac{\sin(\pi(\alpha + \tilde{s}))}{\pi(\alpha + \tilde{s})} {}_1F_1[\tilde{s}; \tilde{s} + \alpha + 1; Z_1] \left[\left(\frac{Z_2}{Z_1} \right)^{\alpha + \tilde{s}} {}_1\tilde{F}_1[-\alpha; -\tilde{s} - \alpha + 1; Z_1] \right. \\ \left. \times ((\alpha + \tilde{s}) {}_1\tilde{F}_1[\tilde{s}; \tilde{s} + \alpha + 1; Z_2] + \tilde{s} Z_2 {}_1\tilde{F}_1[\tilde{s} + 1; \tilde{s} + \alpha + 2; Z_2]) \right. \\ \left. + \alpha Z_2 {}_1\tilde{F}_1[\tilde{s}; \tilde{s} + \alpha + 1; Z_1] {}_1\tilde{F}_1[1 - \alpha; -\tilde{s} - \alpha + 2; Z_2] \right]^{-1}. \quad (C16)$$

- [1] D. R. Cox and H. D. Miller, *The Theory of Stochastic Processes* (CRC Press, London, 1977), Vol. 134.
- [2] C. W. Gardiner, *Handbook of Stochastic Methods*, Springer Series in Synergetics, Vol. 3 (Springer, Berlin, 1985).
- [3] N. G. Van Kampen, *Stochastic Processes in Physics and Chemistry* (Elsevier, 1992), Vol. 1.
- [4] K. L. Drury, Shot noise perturbations and mean first passage times between stable states, *Theor. Pop. Biol.* **72**, 153 (2007).
- [5] B. Leblanc, O. Renault, and O. Scaillet, A correction note on the first passage time of an Ornstein-Uhlenbeck process to a boundary, *Finance Stochast.* **4**, 109 (2000).
- [6] Y. Lin, B. Wu, and Z. Zhang, Determining mean first-passage time on a class of treelike regular fractals, *Phys. Rev. E* **82**, 031140 (2010).
- [7] S. Park, M. K. Sener, D. Lu, and K. Schulten, Reaction paths based on mean first-passage times, *J. Chem. Phys.* **119**, 1313 (2003).
- [8] J. Masoliver, First-passage times for non-Markovian processes: Shot noise, *Phys. Rev. A* **35**, 3918 (1987).
- [9] J. Masoliver and J. M. Porrà, Exact solution to the exit-time problem for an undamped free particle driven by Gaussian white noise, *Phys. Rev. E* **53**, 2243 (1996).
- [10] F. Laio, A. Porporato, L. Ridolfi, and I. Rodriguez-Iturbe, Mean first passage times of processes driven by white shot noise, *Phys. Rev. E* **63**, 036105 (2001).
- [11] G. Calvani, P. Perona, S. Zen, V. Bau', and L. Solari, Return period of vegetation uprooting by flow, *J. Hydrol.* **578**, 124103 (2019).
- [12] G. Capovilla, M. Schmid, and D. Posé, Control of flowering by ambient temperature, *J. Exper. Botany* **66**, 59 (2015).
- [13] J. R. Rigby and A. Porporato, Spring frost risk in a changing climate, *Geophys. Res. Lett.* **35**, L12703 (2008).
- [14] J. M. Rose and D. A. Caron, Does low temperature constrain the growth rates of heterotrophic protists? Evidence and implications for algal blooms in cold waters, *Limnol. Oceanography* **52**, 886 (2007).
- [15] M. Wong and G. Parker, Reanalysis and correction of bed-load relation of Meyer-Peter and Müller using their own database, *J. Hydraulic Engineering* **132**, 1159 (2006).
- [16] E. Weinan and E. Vanden-Eijnden, Transition-path theory and path-finding algorithms for the study of rare events, *Annu. Rev. Phys. Chem.* **61**, 391 (2010).
- [17] N. Zijlstra, D. Nettel, R. Satija, D. E. Makarov, and B. Schuler, Transition path dynamics of a dielectric particle in a bistable optical trap, *Phys. Rev. Lett.* **125**, 146001 (2020).
- [18] S. Condamin and O. Bénichou, Exact expressions of mean first-passage times and splitting probabilities for random walks in bounded rectangular domains, *J. Chem. Phys.* **124**, 206103 (2006).
- [19] N. Levernier, O. Bénichou, and R. Voituriez, Universality classes of hitting probabilities of jump processes, *Phys. Rev. Lett.* **126**, 100602 (2021).
- [20] J. Klinger, R. Voituriez, and O. Bénichou, Splitting probabilities of symmetric jump processes, *Phys. Rev. Lett.* **129**, 140603 (2022).
- [21] G. Botter, A. Porporato, E. Daly, I. Rodriguez-Iturbe, and A. Rinaldo, Probabilistic characterization of base flows in river basins: Roles of soil, vegetation, and geomorphology, *Water Resour. Res.* **43**, W06404 (2007).
- [22] S. Tron, P. Perona, L. Gorla, M. Schwarz, F. Laio, and L. Ridolfi, The signature of randomness in riparian plant root distributions, *Geophys. Res. Lett.* **42**, 7098 (2015).
- [23] P. Perona and B. Crouzy, Resilience of riverbed vegetation to uprooting by flow, *Proc. R. Soc. A* **474**, 20170547 (2018).
- [24] I. Rodriguez-Iturbe, A. Porporato, L. Ridolfi, V. Isham, and D. Coxi, Probabilistic modelling of water balance at a point: The role of climate, soil and vegetation, *Proc. R. Soc. London A* **455**, 3789 (1999).
- [25] E. Daly and A. Porporato, State-dependent fire models and related renewal processes, *Phys. Rev. E* **74**, 041112 (2006).
- [26] M. Abramowitz and I. A. Stegun, *Handbook of Mathematical Functions with Formulas, Graphs, and Mathematical Tables* (US Government Printing Office, Washington, DC, 1964), Vol. 55.
- [27] P. Appell and J. Kampé de Fériet, *Fonctions Hypergeometriques et Hypersphériques: Polynomes d'Hermite* (Gauthier-villars, Paris, 1926).
- [28] L. U. Ancarani and G. Gasaneo, Derivatives of any order of the confluent hypergeometric function ${}_1F_1(a, b, z)$ with respect to the parameter a or b , *J. Math. Phys.* **49**, 063508 (2008).